Preprints.org

Article

Not peer-reviewed version

The Synthesis and Reactivity of Mesoporous and Surface-Rough Vinyl-Containing ORMOSIL Nanoparticles

Nathan I Walton , Eric M Brozek , Courtney C Gwinn , Ilya Zharov *

Posted Date: 27 December 2023

doi: 10.20944/preprints202312.1842.v1

Keywords: organosilica; nanoparticle; mesoporous; vinyl; hydroboration; bromination

Preprints.org is a free multidiscipline platform providing preprint service that is dedicated to making early versions of research outputs permanently available and citable. Preprints posted at Preprints.org appear in Web of Science, Crossref, Google Scholar, Scilit, Europe PMC.

Copyright: This is an open access article distributed under the Creative Commons Attribution License which permits unrestricted use, distribution, and reproduction in any medium, provided the original work is properly cited.

Preprints (www.preprints.org) | NOT PEER-REVIEWED | Posted: 27 December 2023 doi:10.20944/preprints202312.1842.v1

Disclaimer/Publisher's Note: The statements, opinions, and data contained in all publications are solely those of the individual author(s) and contributor(s) and not of MDPI and/or the editor(s). MDPI and/or the editor(s) disclaim responsibility for any injury to people or property resulting from any ideas, methods, instructions, or products referred to in the content.

Article

The Synthesis and Reactivity of Mesoporous and Surface-Rough Vinyl-Containing ORMOSIL Nanoparticles

Nathan I. Walton, Eric M. Brozek, Courtney C. Gwinn and Ilya Zharov *

Department of Chemistry, University of Utah, 315 South 1400 East, Salt Lake City, UT 84112, USA
* Correspondence: i.zharov@utah.edu

Abstract: Silica nanoparticles synthesized solely from organosilanes naturally possess a greater number of organic functionalities than silica nanoparticles surface modified with organosilanes. We report the synthesis of organically modified silica (ORMOSIL) nanoparticles with mesoporous and surface rough morphology and with high surface area, made solely from vinyltrimethoxy silane. We chemically modified these vinyl silica nanoparticles using bromination and hydroboration, and demonstrated the high accessibility and reactivity of the vinyl groups with an ~85% conversion of the functional groups for bromination of both particle types, a ~60% conversion of the functional groups for hydroboration of surface rough particles and a 90% conversion of the functional groups for hydroboration of mesoporous particles. We determined that the mesoporous vinyl silica nanoparticles, while having a surface area that lies between the non-porous and surface rough vinyl silica nanoparticles, provide the greatest accessibility to the vinyl groups for boronation and allow incorporating up to 3.1×10^6 B atoms per particle, making the resulting materials attractive for boron neutron capture therapy.

Keywords: organosilica; nanoparticle; mesoporous; vinyl; hydroboration; bromination

1. Introduction

The chemical and thermal robustness, combined with the hydrophilicity of silica nanoparticles, render them effective carriers for diverse organic and inorganic substances [**Error! Reference source not found.**]. They hold significant promise for uses in optical, imaging, and therapeutic applications [**Error! Reference source not found.**]. Mesoporous organosilica nanoparticles represent an even more interesting but much less studied class of materials [**Error! Reference source not found.**,**Error! Reference source not found.**]. While silica inherently has only the silanol reactive groups, the introduction of organosilanes gives them beneficial organic features [**Error! Reference source not found.**]. They combine the properties of organic and silica materials and have emerged as a class of hybrid materials with diverse potential applications in catalysis, drug delivery, imaging, and more. Organosilanes can alter the surface charge and polarity of these nanoparticles, and offer options for further modifications using conventional synthesis methods [**Error! Reference source not found.**].

Silica nanoparticles with mesopores in the range of 2-30 nm are commonly prepared by the condensation of silica precursors (silica alkoxides TEOS, TMOS [7–9], their functionalized derivatives [**Error! Reference source not found.**], sodium silicates [**Error! Reference source not found.**]) in the presence of surfactant micelles and a catalyst in an aqueous medium [**Error! Reference source not found.**]. This process is affected by the surfactant concentration [**Error! Reference source not found.**,**Error! Reference source not found.**], the type and amount of hydrolyzing agents [7,8,15–23] the presence of various kosmotropic and chaotropic salts [12,24–35]. alcohol additives [8,9,36–39] and the degree of dilution [**Error! Bookmark not defined.**,**Error! Bookmark not defined.**,**Error! Bookmark not defined.**,**Error! Reference source not found.**].

Two techniques exist to incorporate organic functional groups within silica: "grafting to" and co-condensation [**Error! Reference source not found.**]. In the "grafting to" method, silica nanoparticles

© 2023 by the author(s). Distributed under a Creative Commons CC BY license.

Preprints (www.preprints.org) | NOT PEER-REVIEWED | Posted: 27 December 2023 doi:10.20944/preprints202312.1842.v1

are modified after creation through a reaction that uses an organosilane, causing a hydrolysis/condensation process. This not only maintains the nanoparticle's initial shape but also adds organic functions to its surface. A series of organic layers can be incorporated due to the ability of organosilanes to introduce new groups which can partake in more condensation. For monolayers, the number of organic groups on the surface depends on the number of available silanol groups (~3-5 Si-OH per nm2). Still, organosilane condensation often results in more comprehensive surface coverage [**Error! Reference source not found.**].

The co-condensation technique offers organically modified silica (ORMOSIL) nanoparticles infused with organic functionalities distributed throughout their structure. While this leads to a larger count of organic groups, they can be hard to modify later, typically necessitating prior selection (e. g., covalent encapsulation of a fluorophore) [**Error! Reference source not found.**,**Error! Reference source not found.**]. Mostly, only those organic functional groups on the silica exterior are accessible and apparently abundant in both methods.

Emerging techniques aim to increase the ratio of the silica nanoparticles' surface area to volume, hence enhancing the organic functions' accessibility or quantity. This involves the creation of particles with rough surfaces or mesoporous structures [**Error! Reference source not found.**,**Error! Reference source not found.**]. Despite both types of particles possessing extensive surface areas, their utility differs vastly. Rough surface silica nanoparticles are prepared either by etching the silica particles [**Error! Reference source not found.**] or incorporating smaller spheres onto bigger ones [**Error! Bookmark not defined.**]. When merged with water-repelling organosilanes, these nanoparticles adopt very hydrophobic traits, proving useful in the production of water-repellent glass [**Error! Reference source not found.**,**Error! Reference source not found.**].

On the other hand, mesoporous particles are produced using a solution where micelles direct the silica formation [**Error! Reference source not found.**]. This offers a higher surface area and silanol group availability, paving the way for added modifications. In these nanoparticles, the mesoporous structure grants more organic group access via the pores. Consequently, these particles have been applied in drug delivery [**Error! Reference source not found.**,**Error! Reference source not found.**] and imaging [53–55] due to their ability to encapsulate therapeutic and/or imaging agents.

Increasing the number of organic functional groups can enhance the usefulness of silica nanoparticles. Thus, preparing such particles solely from functional organosilanes would be advantageous. In such particles, the organic functions become more accessible as the silica framework becomes altered due to replacing the Si-O bonds with bonds to organic groups, and due to steric factors, leading to some porosity [**Error! Reference source not found.**]. Like traditional particles, enhancing these nanoparticles' surface area by adding mesopores can amplify the organic functions' accessibility even further. Yet, preparing these nanoparticles remains a challenge, with the organically modified silica nanoparticle domain still budding in silica chemistry [**Error! Reference source not found.**,**Error! Reference source not found.**].

ORMOSIL nanoparticles containing vinyl groups are of interest because these functional groups can undergo further transformations using well-established alkene reactions, such as to bromination, hydroxylation and hydroboration [**Error! Bookmark not defined.**]. The result of the latter are nanoparticles containing large amounts of boron, which constitute attractive agents for boron neutron capture therapy (BNCT) of cancer, the process where ^{10}B nuclei undergo a localized fission reaction and emit alpha particles capable of destroying cancer cells [**Error! Reference source not found.**].

Our research on the preparation of organosilica nanoparticles initially focused on the synthesis of the particles incorporating reactive functional groups using co-condensation of organosilanes with tetraethoxysilane. For example, we prepared [**Error! Bookmark not defined.**] non-porous vinylsilsesquioxane nanoparticles and showed that the vinyl groups inside the nanoparticles can be easily brominated or hydroborated, leading to the nanoparticles containing 59.9 wt% of bromine or 3.6 wt% of boron, respectively. We also designed, prepared, and characterized [**Error! Reference source not found.**] hydrolysable organosilica nanoparticles (ICPTES-Sorbitol SNPs) by co-condensation of tetraethoxysilane with a bridged sorbitol-based silsesquioxane precursor containing

Preprints (www.preprints.org) | NOT PEER-REVIEWED | Posted: 27 December 2023 doi:10.20944/preprints202312.1842.v1

carbamate linkages. We later shifted our focus to a novel method for the preparation of mesoporous particles [**Error! Reference source not found.**] and to the preparation of organosilica nanoparticles using organosilanes as sole precursors [**Error! Reference source not found.**]. We also prepared [**Error! Reference source not found.**,**Error! Reference source not found.**] organosilica nanoparticles with internal metal-chelating diethylenetriametetraacetic acid groups (DTTA-MSNPs) by co-condensation and studied the binding of transition metal ions such as copper(II), cobalt (II) and gadolinium (III) by DTTA-MSNPs.

Given the importance of ORMOSIL nanoparticles, particularly those with mesopores and with reactive organic functional groups, and the limited synthetic approaches available for their preparation, we decided to explore the preparation of such particles further. Our current paper describes the results of our efforts, namely two synthetic methods for the preparation of novel large surface area vinyl ORMOSIL nanoparticles using the corresponding organosilane as a sole precursor. These methods use micellar solutions to create mesoporous and surface rough nanoparticles. The paper also describes organic transformations of the vinyl groups inside the porous and surface rough ORMOSIL nanoparticles, and the results are compared to determine the extent of vinyl group transformation.

2. Materials and Methods

Materials. The following materials were used as received, vinyltrimethoxy silane (VTMS, 97%, Gelest Inc.), hexadecyltrimethylammonium bromide (CTAB, 99.0%, Sigma-Aldrich), mesitylene (1,3,5-trimethylbenzene, TMB, 97%, Sigma-Aldrich), ethylene glycol (EG, 99%, Macron Chemicals), ammonium hydroxide (28-30%, Sigma-Aldrich), 1 M borane in tetrahydrofuran (Sigma-Aldrich), bromine (Sigma-Alrich), hydrochloric acid (concentrated, Fluka) and ethanol (anhydrous, Decon Labs).

Instruments. Transmission electron microscopy was performed using FEI Techna G2 T-12 microscope with an acceleration voltage of 120 kV. Average particle size and standard deviation were calculated from measuring 150-250 particles using the ImageJ software. FT-IR spectroscopy was performed using Bruker Tensor 37. Nitrogen adsorption-desorption analysis was performed using Micrometrics ASAP 2020. The degassing procedure was carried out at 200 °C for 4 h under 1 μm Hg vacuum, and the isotherm was recorded in the pressure range of P/P_o=0.002-0.99. The specific surface areas were calculated using the multipoint BET method at P/P_o=0.05-0.25, the pore size distributions – by BJH (cylindrical pores) on the adsorption branch of the isotherm. Thermogravimetric analysis was performed using Instruments 2950 Thermogravimetric Analyzer for vacuum-dried particles at a heating rate of 10 °C/min from room temperature to 800 °C. The percent of the vinyl groups was calculated using the following equation:

$$\frac{\rho \cdot \frac{4}{3} \cdot \pi \cdot r_{(cm)}{}^3 \cdot \%W_{loss_{vSNP}}}{100 \cdot MW_{vinyl}} = \frac{\text{mol vinyl}}{\text{particle}}$$

where ϱ is the particle density in g·cm^{-3} (~1.35), r is the particle radius, MW_{vinyl} is the molecular weight of vinyl group, and $\%W_{loss}$ is the TGA measured weight loss of the vSNPs. The percent conversion of the vinyl groups was calculated using the following equation:

$$\frac{\rho \cdot \frac{4}{3} \cdot \pi \cdot r_{(cm)}{}^3 \cdot (\%W_{loss_{VNP+X}} - \%W_{loss_{VNP}})}{100 \cdot MW_X} = \frac{\text{mol X}}{\text{particle}}$$

where ϱ is the particle density in g·cm^{-3} (~1.35), r is the particle radius, MW_X is the molecular weight of vinyl group, and $\%W_{loss}$ is the TGA measured weight loss of the nanoparticles. The percentage of vinyl groups reacted in bromination or hydroboration was calculated using the following equation:

$$\frac{\text{mol X}}{\text{particle}} \div \frac{\text{mol vinyl}}{\text{particle}} \times 100 = \text{mol \% conversion}$$

Mesoporous vinyl silica nanoparticle synthesis. CTAB (0.587 g, 1.61 mmol), ethanol (43 mL), EG (15 mL) and 28% NH_4OH (3.6 mL) were dissolved in 90 mL MilliQ water in a 250 mL round bottom flask. The solution was stirred rapidly at 70 °C for 25 minutes. VTMS (0.69 mL, 3.2 mmol) was added to the solution which was stirred for 72 hours at room temperature. The resulting particles were collected by centrifugation and washed 3 times with 10 mL of ethanol. The particles were then

Preprints (www.preprints.org) | NOT PEER-REVIEWED | Posted: 27 December 2023 doi:10.20944/preprints202312.1842.v1

added to 30 mL of the ethanolic solution of 1 M HCl in a 100 mL round bottom flask and heated at 80 °C for 12 hours to remove the CTAB. The particles were collected and washed 3 times with 10 mL of ethanol.

Surface rough vinyl silica nanoparticle synthesis. CTAB (0.587 g, 1.61 mmol), TMB (0.66 mL, 4.74 mmol, 2.95:1 TMB:CTAB), EG (15 mL), ethanol (43 mL) and 28% NH_4OH (3.6 mL) were dissolved in 90 mL MilliQ water in a 250 mL round bottom and were stirred rapidly at 70 °C for 25 minutes. VTMS (0.69 mL, 3.2 mmol) was then added to the solution which was stirred for 72 hours at room temperature. The resulting particles were collected by centrifugation and washed 3 times with 10 mL of ethanol. The particles were then added to 30 mL of the ethanolic solution of 1 M HCl in a 100 mL round bottom flask and heated at 80 °C for 12 hours to remove the CTAB. The particles were collected and washed 3 times with 10 mL of ethanol.

Table 1. Characteristics of synthesizes nanoparticles.

Particles	Size, nm	Surface area, $m^2 \cdot g^{-1}$	Calculated pore size, nm
mVSNPs	137 ± 8	44.0	37-50
rVSNPs	97 ± 6	278.7	18*
sVSNPs	592 ± 18	8.5	0

* Due to surface roughness rather than "through-and-through" pores.

Bromination of vinyl silica particles. Vinyl silica nanoparticles (0.1 g, 1.25 mmol) were placed in a scintillation vial containing 10 mL of dichloromethane and sonicated until the particles were well-dispersed. Bromine (0.19 mL, 3.75 mmol) was added to the solution followed by brief sonication. The reaction mixture was stirred overnight at room temperature. The particles were collected via centrifugation and washed five times with 10 mL of dichloromethane to completely remove the bromine.

Hydroboration of vinyl silica particles. Under the nitrogen atmosphere, vinyl silica nanoparticles (0.1 g) were placed in 5 mL of 1 M $BH_3 \cdot THF$ (5 mL) in a 25 mL round bottom flask and 6 mL of THF were added. The reaction mixture was stirred for 3 hours, sonicated and then stirred again overnight at room temperature. The particles were then collected and washed three times with 10 mL of THF to remove excess $BH_3 \cdot THF$, followed by washing with a 9:1 ethanol-water mixture and sonication in 10 mL of MilliQ water to complete the conversion to boric acids. Finally, the particles were washed twice with 10 mL of MiliQ water.

3. Results and Discussion

Synthesis of vinyl containing ORMOSIL nanoparticles. There is a limited number of organosilane precursors currently known to produce ORMOSIL nanoparticles [**Error! Reference source not found.**]. Among them, the vinyltrimethoxy silane (VTMS) is noteworthy, especially given its ability to hydrolyze and condense under the Stöber conditions [**Error! Reference source not found.**].

By introducing cetyltrimethylammonium bromide (CTAB) and ethylene glycol to VTMS, we successfully prepared mesoporous vinyl silica nanoparticles (mVSNP). CTAB is responsible for micelle formation which then results in mesopore creation, while ethylene glycol augments solution viscosity. This aids in silica nuclei production, controlling particle dimensions and ensuring consistency. The concentrations of ethylene glycol, water, and ethanol greatly influence mVSNP generation [**Error! Reference source not found.**].

We identified certain conditions hindering the mVSNP formation. Without an optimal ethanol/water ratio or insufficient reaction duration (less than 72 hours), the particles either are not formed, or a gel is produced. The gel is also produced if ethanol is added after VTMS. At reaction temperature below 50 °C, the resulting porosity was also significantly reduced.

Transmission Electron Microscopy (TEM) revealed porous spherical mVSNPs with an average particle diameter of 137 ± 8 nm and with pores of varied sizes randomly distributed throughout the ORMOSIL particle structure (Figure 1A-B). The fluctuating pore dimensions might be attributed to

Preprints (www.preprints.org) | NOT PEER-REVIEWED | Posted: 27 December 2023 doi:10.20944/preprints202312.1842.v1

the VTMS precursor interacting with the hydrophobic core of the micelles, potentially explaining the lower yield, especially if pore interconnection happens during synthesis.

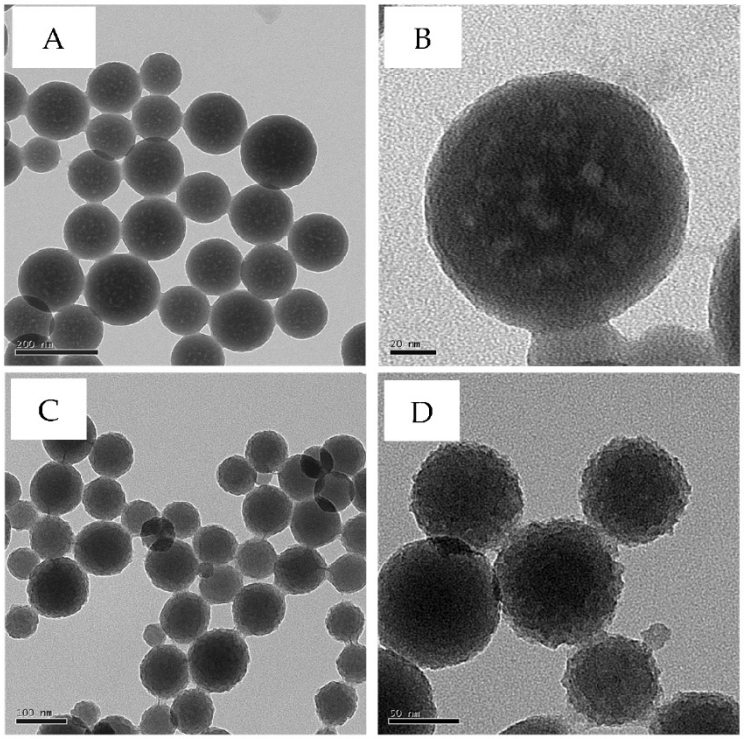

Figure 1. TEM images of mVSNPs (A-B) and rVSNPs (C-D). Scale bars are 200 nm (A), 20 nm (B), 100 nm (C) and 50 nm (D).

An example of the mVSNPs nitrogen sorption isotherm is shown in Figure 2A. This isotherm has an expected large nitrogen absorption (~260 cm3·g-1 STP) and appears to be type II. How-ever, it has an H1 hysteresis loop between 0.92 to 1 P/Po, indicating mesoporosity, and therefore, it is probably a type IV without the noticeable plateau, which is not uncom-mon for mesoporous materials [45,68]. Although the large nitrogen absorption and hysteresis loop are indicative of a mesoporous material, the pore diameter measure-ment had a wide distribution of sizes from the 2 nm to 300 nm. This broad size range can be explained by a combination of micropores (< 2 nm), mesopores (2- 50 nm), some of which may be connected, and voids created by particle aggregation. The pore size distribution showed the periodic pore size maxima from 2 nm to ~ 30 nm (2, 7, 12, 18, and 23 nm) demonstrating that the mesopores are not uniform in size. According to BJH calculations, the mVSNPs have the average pore sizes between 37 and 50 nm. This pore size agrees with the pore sizes observed by TEM. BET analysis of the mVSNP samples gave the surface area of mVSNP in the range of 30.3-44.0 m2·g-1. This surface area is 3.5-5 times larger than that of non-porous sVSNPs, which are discussed below. However, this surface area is lower than that for other reported mesoporous silica par-ticles [29]. Given the large size of the pores in mVSNP, the overall lower surface area means that these particles possess a lower pore density.

When trimethylbenzene (TMB), a swelling agent, was added before VTMS condensation, we expected the formation of particles with larger pores. Instead, we produced surface-rough particles (rVSNPs, Figure 1C-D), possibly because VTMS could not fully envelop the expanded micelles. However, the yield of these rough-surfaced particles was higher, perhaps owing to TMB's interaction with VTMS within the micelles. The size of these rVSNPs was 97 ± 6 nm and their nitrogen absorption isotherm (Figure 2B) gave a nitrogen adsorption of ~450 $cm^3 \cdot g^{-1}$, which is higher than that of mVSNPs. Based on the absence of a "loop" in the hysteresis of the nitrogen sorption isotherm of rVSNPs as opposed to mVSNP, we concluded that rVSNPs contain porous areas with hindered nitrogen exchange. According to BJH calculations, the size of the pores in rVSNPs is 18.5 nm. This observation

Preprints (www.preprints.org) | NOT PEER-REVIEWED | Posted: 27 December 2023 doi:10.20944/preprints202312.1842.v1

is likely due to the cavities created by the rough surface because if there were "through-and-through" pores of this calculated size, they would be visible by TEM. Finally, the BET surface area of rVSNPs was determined to be 278.70 $m^2 \cdot g^{-1}$, significantly larger than that of mVSNPs. Taken together, our observations from TEM and BET suggest that rVSNPs are mostly non-porous with their morphology and properties defined by their rough surface.

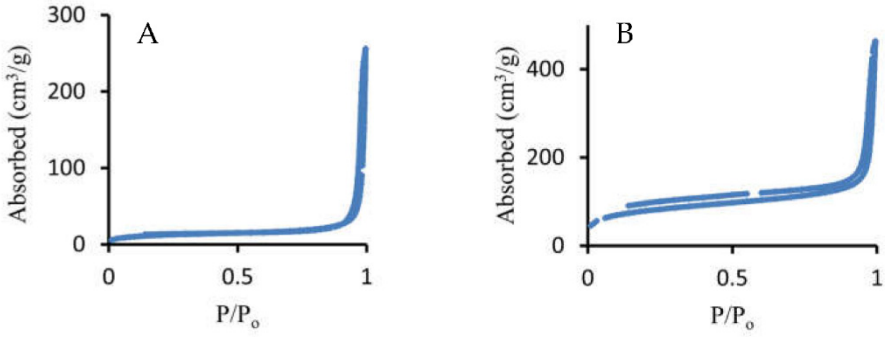

Figure 2. Nitrogen adsorption-desorption isotherms of mVSNPs (A) and rVSNPs (B).

For comparison, non-porous vinyl silica nanoparticles (sVSNPs) were also produced without CTAB. These particles were larger and lacked porosity, with a distinct nitrogen absorption profile. Specifically, the diameter of sVSNPs was 592 ± 18 nm, their BET surface area was 8.48 m2·g−1 and they showed type II isotherm, all characteristic of non-porous materials [**Error! Reference source not found.**].

Bromination of vinyl silica nanoparticles. Bromination was our chosen model reaction, given the ease with which bromine reacts with alkenes. Upon brominating the vinyl particles (Scheme 1), the characteristic color of bromine vanished, producing a pale powder. To confirm that the bromination indeed took place, we used IR spectroscopy (Figure 3). We observed that the vinyl group stretch at 960 cm−1 disappeared and the 1602 cm−1 stretch was greatly reduced. We also observed new bands at 875, 760 and 650 cm−1, which correspond to C-Br stretches.

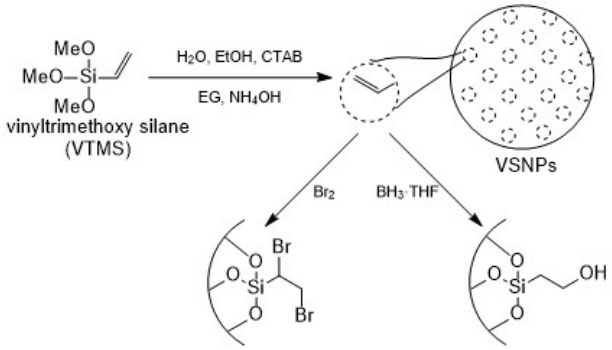

Scheme 1. Preparation and chemical modification of vinyl-containing nanoparticles.

Preprints (www.preprints.org) | NOT PEER-REVIEWED | Posted: 27 December 2023 doi:10.20944/preprints202312.1842.v1

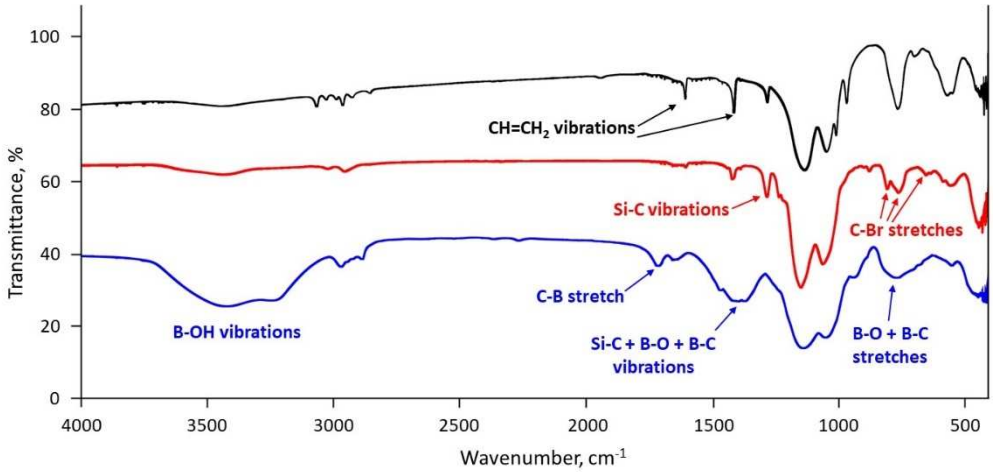

Figure 3. IR spectra of unmodified (black), brominated (red), and hydroborated (blue) mVSNPs.

Thermogravimetric analysis (TGA) further confirmed the extensive bromination of the vinyl groups in the prepared nanoparticles. All three types of nanoparticles, sVSNP, rVSNPs and mVSNPs, exhibited weight loss of ~60% after their bromination (Figure 4). This is significantly higher compared to the weight loss of ~9% observed for these particles before the bromination. Using the TGA weight loss for sVSNP, rVSNPs and mVSNPs we calculated the percent conversion of the vinyl groups in the bromination reaction to be ~85%. This result suggests that (1) the vinyl groups in all three types of the prepared nanoparticles are accessible and highly reactive, and (2) the accessibility of the vinyl groups to bromine and their reactivity with bromine in all three types of the prepared nanoparticles is similar.

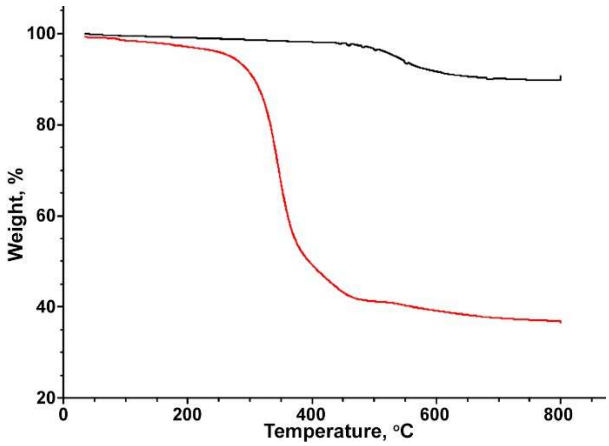

Figure 4. TGA weight loss of mVSNPs (black) and brominated mVSNPs (red).

Hydroboration of vinyl silica nanoparticles. To explore potential uses for ORMOSIL particles in Boron Neutron Capture Therapy (BNCT), we performed the hydroboration of VSNPs using BH_3·THF. Infrared spectroscopy (Figure 3) confirmed successful hydroboration, indicating significant chemical changes within the particles. Specifically, the Si-C stretch at 1410 cm^{-1} broadened after hydroboration likely due to the appearance of B-O vibrations in the same region. A new band at 770 cm^{-1} appeared, corresponding to O-B-O and/or B-C stretches. Another new band, at 3500 cm^{-1}, indicated the formation of hydroxyl groups belonging to boric acid. Finally, a new band appeared at 1712 cm^{-1}, corresponding to the C-B-C stretch. Based on these observations, we concluded that the vinyl groups inside VNSPs indeed underwent hydroboration and were converted to boric acid. This reaction also led to a marked difference in particle solubility, with hydroborated particles becoming hydrophilic unlike the starting particles, which are only dispersible in hexane.

Preprints (www.preprints.org) | NOT PEER-REVIEWED | Posted: 27 December 2023 doi:10.20944/preprints202312.1842.v1

A TGA-based comparative study revealed the degree of hydroboration among various VSNP particles. For sVSNPs and rVSNPs, TGA showed a weight loss of ~9% before the hydroboration. After the hydroboration, the weight loss increased to ~19% for sVSNPs and to ~18% for rVSNPs (Figure 5). Using these results, the conversion of the vinyl groups to boric acid by hydroboration is calculated to be ~58% for sVSNPs and ~56% for rVSNPs. The resulting boron content is 1.69×10^{21} B·cm^{-3} (1.8×10^{8} B per particle) for sVSNPs and 1.56×10^{21} B·cm^{-3} (7.2×10^{5} B per particle) for rVSNPs. Therefore, sVSNPs and rVSNPs showed very similar behavior in terms of their hydroboration.

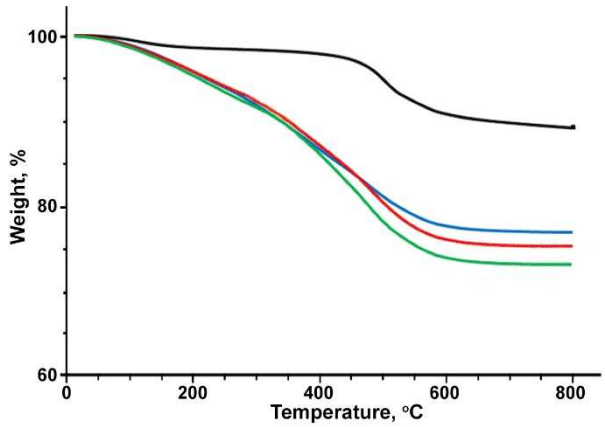

Figure 5. TGA weight loss of unmodified sVSNPs (black) and hydroborated sVSNPs (red), rVSNPs (blue), and mVSNPs (green).

In contrast, for mVSNPs TGA showed a higher weight loss of ~22% (Figure 5), which corresponds to a significantly higher extent of vinyl group conversion to boric acid, at ~90%, or ca. 1.5 times greater than that for sVSNPs or rVSNPs. This also leads to a significantly higher boron loading after the hydroboration of mVSNPs, at 2.3×10^{21} B·cm^{-3} (3.1×10^{6} B per particle). We hypothesize that this is the result of the presence of mesopores in mVSNPs that should facilitate the access of the hydroboration agent to the vinyl groups throughout the mVSNP structure. Interestingly, we did not observe such selectivity in the case of bromination, where all three types of prepared nanoparticles showed similar degrees of vinyl groups conversion (85%). This is likely due to the much higher reactivity of bromine towards the double bonds, compared to that of BH_3·THF.

4. Conclusions

We developed the synthesis of ORMOSIL nanoparticles with large surface areas and high content of vinyl functional groups from vinyltrimethoxy silane as a sole precursor. By using a surfactant (CTAB), we created vinyl-containing nanoparticles with mesopores in 37-50 nm range. When a swelling agent (TMB) was introduced to the reaction mixture, surface-rough vinyl particles (rather than mesoporous particles with larger pores) were formed. Both particle types possess high surface area and abundant reactive vinyl groups that can be undergo bromination and hydroboration, achieving high conversion of the vinyl groups. The hydroborated particles can potentially be used as efficient boron carriers for BNCT applications, containing approximately 10^{6} boron atoms per particle.

Acknowledgments: This work was supported by an Energy Frontier Research Center EFRC-MUSE funded by the US Department of Energy, Office of Science, Basic Energy Sciences, Award #DE-SC0019285.

Preprints (www.preprints.org) | NOT PEER-REVIEWED | Posted: 27 December 2023 doi:10.20944/preprints202312.1842.v1

References

1. Jeelani, P. G.; Mulay, P.; Venkat, R.; Ramalingam, C. Multifaceted application of silica nanoparticles. A review. *Silicon* **2020**, *12*, 1337-1354.
2. Croissant, J. G.; Fatieiev, Y.; Almalik, A.; Khashab, N. M. Mesoporous silica and organosilica nanoparticles: physical chemistry, biosafety, delivery strategies, and biomedical applications. *Adv. Healthcare Mater.* **2018**, 7, 1700831.
3. Guan, B.; Cui, Y.; Ren, Z.; Qiao, Z. A.; Wang, L.; Liu, Y.; Huo, Q. Highly Ordered Periodic Mesoporous Organosilica Nanoparticles With Controllable Pore Structures. *Nanoscale* **2012**, *4*, 6588-6596.
4. Teng, Z.; Li, W.; Tang, Y.; Elzatahry, A.; Lu, G.; Zhao, D. Mesoporous Organosilica Hollow Nanoparticles: Synthesis And Applications. *Adv. Mater.* **2019**, ***31***, 1707612.
5. Zou, H.; Ren, Y. Synthetic strategies for nonporous organosilica nanoparticles from organosilanes. *Nanoscale* **2023**, *15*, 10484-10497.
6. Jin, Y.; Li, A.; Hazelton, S. G.; Liang, S.; John, C. L.; Selid, P. D.; Pierce, D. T.; Zhao, J. X. Amorphous silica Nanohybrids: Synthesis, Properties and Applications. *Coord. Chem. Rev.* **2009**, *253*, 2998-3014.
7. Qiao, Z. A.; Zhang, L.; Guo, M.; Liu, Y.; Huo, Q. Synthesis Of Mesoporous Silica Nanoparticles Via Controlled Hydrolysis And Condensation Of Silicon Alkoxide. *Chem. Mater.* **2009**, *21*, 3823-3829.
8. Yano, K.; Fukushima, Y. Synthesis Of Mono-Dispersed Mesoporous Silica Spheres With Highly Ordered Hexagonal Regularity Using Conventional Alkyltrimethylammonium Halide As A Surfactant. *J. Mater. Chem.* **2004**, *14*, 1579-1584.
9. Yamada, H.; Urata, C.; Ujiie, H.; Yamauchi, Y.; Kuroda, K. Preparation Of Aqueous Colloidal Mesostructured And Mesoporous Silica Nanoparticles With Controlled Particle Size In A Very Wide Range From 20 nm to 700 nm. *Nanoscale* **2013**, *5*, 6145-6153.
10. Croissant, J. G.; Fatieiev, Y.; Khashab, N. M. Degradability and Clearance of Silicon, Organosilica, Silsesquioxane, Silica Mixed Oxide, and Mesoporous Silica Nanoparticles. *Adv. Mater.* **2017**, *29*, 1604634.
11. Lin, H. P.; Tsai, C. P. Synthesis of Mesoporous Silica Nanoparticles from a Low-concentration CnTMAX-Sodium Silicate Components. *Chem. Lett.* **2003**, *32*, 1092-1093.
12. Wan, Y.; Zhao, D. On The Controllable Soft-Templating Approach To Mesoporous Silicates. *Chem. Rev.* **2007**, *107*, 2821-2860.
13. Lelong, G.; Bhattacharyya, S.; Kline, S.; Cacciaguerra, T.; Gonzalez, M. A.; & Saboungi, M. L. Effect Of Surfactant Concentration On The Morphology And Texture Of MCM-41 Materials. *J. Phys. Chem. C* **112**, 10674-10680 (2008).
14. Chen, B.; Wang, Z.; Quan, G.; Peng, X.; Pan, X.; Wang, R.; Xu, Y.; Li, G.; Wu, C. In Vitro And In Vivo Evaluation Of Ordered Mesoporous Silica As A Novel Adsorbent In Liquisolid Formulation. *Int. J. Nanomed.* **7**, 199-209 (2012).
15. Möller, K.; Bein, T. Talented Mesoporous Silica Nanoparticles. *Chem. Mater.* **2017**, *29*, 371-388.
16. Li, X.; Li, X.; Shi, B.; Chaikittisilp, W.; Li, M.; Wang, Y.; Liu, Y.; Gao, L.; Mao, L. A General Method To Synthesize A Family Of Mesoporous Silica Nanoparticles Less Than 100 nm And Their Applications In Anti-Reflective/Fogging Coating. *J. Mater. Sci.* **2016**, *51*, 6192-6206.
17. Cai, Q.; Luo, Z. S.; Pang, W. Q.; Fan, Y. W.; Chen, X. H.; Cui, F. Z. Dilute Solution Routes to Various Controllable Morphologies of MCM-41 Silica with a Basic Medium. *Chem. Mater.* **2001**, *13*, 258-263.
18. Lai, C. Y.; Trewyn, B. G.; Jeftinija, D. M.; Jeftinija, K.; Xu, S.; Jeftinija, S.; Lin, V. S. Y. A Mesoporous Silica Nanosphere-Based Carrier System with Chemically Removable CdS Nanoparticle Caps for Stimuli-Responsive Controlled Release of Neurotransmitters and Drug Molecules. *J. Am. Chem. Soc.* **2003**, *125*, 4451-4459.
19. Liu, J.; Li, C.; Li, F. Fluorescence Turn-On Chemodosimeter-Functionalized Mesoporous Silica Nanoparticles and Their Application in Cell Imaging. *J. Mater. Chem.* **2011**, *21*, 7175-7181.
20. Lu, F.; Wu, S. H.; Hung, Y.; Mou, C. Y. Size Effect on Cell Uptake in Well-Suspended, Uniform Mesoporous Silica Nanoparticles. *Small* **2009**, *5*, 1408-1413.
21. Lin, Y. S.; Tsai, C. P.; Huang, H. Y.; Kuo, C. T.; Hung, Y.; Huang, D. M.; Chen, Y. C.; Mou, C. Y. Well-Ordered Mesoporous Silica Nanoparticles as Cell Markers. *Chem. Mater.* **2005**, *17*, 4570-4573.
22. Yokoi, T.; Karouji, T.; Ohta, S.; Kondo, J. N.; Tatsumi, T. Synthesis of Mesoporous Silica Nanospheres Promoted by Basic Amino Acids and Their Catalytic Application. *Chem. Mater.* **2010**, *22*, 3900-3908.
23. Zhang, K.; Xu, L. L.; Jiang, J. G.; Calin, N.; Lam, K. F.; Zhang, S. J.; Wu, H. H.; Wu, G. D.; Albela, B.; Bonneviot, L.; Wu, P. Facile Large-Scale Synthesis of Monodisperse Mesoporous Silica Nanospheres with Tunable Pore Structure. *J. Am. Chem. Soc.* **2013**, *135*, 2427-2430.
24. Lin, H. P.; Mou, C. Y. Structural and Morphological Control of Cationic Surfactant-Templated Mesoporous Silica. *Acc. Chem. Res.* **2002**, *35*, 927-935.
25. Xiang, W. D.; Yang, Y. X.; Zheng, J. L.; Cao, L.; Ding, H. J.; Liu, X. N. Synthesis of Mesoporous Silica by Cationic Surfactant Templating in Various Inorganic Acid Sources. *Mater. Sci. Pol.* **2010**, *28*, 709-730.
26. Bagshaw, S. A. The Effect of Dilute Electrolytes on the Formation of Non-Ionically Templated [Si]-MSU-X Mesoporous Silica Molecular Sieves. *J. Mater. Chem.* **2001**, *11*, 831-840.

Preprints (www.preprints.org) | NOT PEER-REVIEWED | Posted: 27 December 2023 doi:10.20944/preprints202312.1842.v1

27. Lin, H. P.; Kao, C. P.; Mou, C. Y.; Liu, S. B. Counterion Effect in Acid Synthesis of Mesoporous Silica Materials. *J. Phys. Chem. B* **2000**, *104*, 7885-7894.
28. Li, Y.; Wang, Y.; Huang, G.; Ma, X.; Gao, I. A Surprising Chaotropic Anion-Induced Supramolecular Self-Assembly of Ionic Polymeric Micelles. *Angew. Chem. Int. Ed.* **2014**, *53*, 8074-8078.
29. Yu, C.; Fan, J.; Tian, B.; Zhao, D.; Stucky, G. D. High-Yield Synthesis of Periodic Mesoporous. *Adv. Mater.* **2002**, *14*, 1742-1745.
30. Issa, A. A.; Luyt, A. S. Kinetics of Alkoxysilanes and Organoalkoxysilanes Polymerization: A Review. *Polymers* **2019**, *11*, 537.
31. Yu, C.; Tian, B.; Fan, J.; Stucky, G. D.; Zhao, D. Salt Effect in the Synthesis of Mesoporous Silica Templated by Non-Ionic Block Copolymers. *Chem. Commun.* **2001**, *24*, 2726-2727.
32. Yu, C.; Fan, J.; Tian, B.; Zhao, D. Morphology Development of Mesoporous Materials: A Colloidal Phase Separation Mechanism. *Chem. Mater.* **2004**, *16*, 889-898 (2004).
33. Trompette, J. L. Influence of Co-Ion Nature on the Gelation Kinetics of Colloidal Silica Suspensions. *J. Phys. Chem. B* **2017**, *121*, 5654-5659.
34. Van Der Linden, M. Conchúir, B. O.; Spigone, E.; Niranjan; A., Zaccone, A.; Cicuta, P. Microscopic Origin of the Hofmeister Effect in Gelation Kinetics of Colloidal Silica. *J. Phys. Chem. Lett.* **2015**, *6*, 2881-2887 (2015).
35. Tadros, T. F.; Lyklema, J. Adsorption of Potential-Determining Ions at the Silica-Aqueous Electrolyte Interface and the Role of Some Cations. *J. Electroanal. Chem. Interfacial Electrochem.* **1968**, *17*, 267-275.
36. Matsoukas, T.; Gulari, E. Dynamics of Growth of Silica Particles from Ammonia-Catalyzed Hydrolysis of Tetra-Ethyl-Orthosilicate. *J. Colloid Interface Sci.* **1988**, *124*, 252-261.
37. Zainal, N. A.; Shukor, S. R. A.; Wab, H. A. A.; Razak, K. A. Study on the Effect of Synthesis Parameters of Silica Nanoparticles Entrapped with Rifampicin. *Chem. Eng. Trans.* **2013**, *32*, 2245-2250.
38. Issa, A. A.; El-Azazy, M.; Luyt, A. S. Kinetics of alkoxysilanes hydrolysis: An empirical approach. *Sci. Rep.* **2019**, *9*, 1-15.
39. Yamada, Y.; Yano, K. Synthesis of Monodispersed Super-Microporous/Mesoporous Silica Spheres with Diameters in the Low Submicron Range. *Micropor. Mesopor. Mater.* **2006**, *93*, 190-198.
40. Gu, J.; Huang, K.; Zhu, X.; Li, Y.; Wei, J.; Zhao, W.; Liu, C.; Shi, J. Sub-150 nm Mesoporous Silica Nanoparticles with Tunable Pore Sizes and Well-Ordered Mesostructure for Protein Encapsulation. *J. Colloid Interface Sci.* **2013**, *407*, 236-242.
41. Yang, B.; Chen, Y.; Shi, J. Mesoporous silica/organosilica nanoparticles: Synthesis, biological effect and biomedical application. *Mater. Sci. Engineering R* **2019**, *137*, 66-105.
42. Brauer, F.; Gläsel, H-J.; Decker, U.; Ernst, H.; Freyer, A.; Hartmann, E.; Sauerland, V.; Mehnert, R. Trialkoxysilane grafting onto nanoparticles for the preparation of clear coat polyacrylate systems with excellent scratch performance. *Prog. Org. Coatings* **2003**, *47*, 147-153.
43. Wang, L.; Tan, W. Multicolor FRET silica nanoparticles by single wavelength excitation. *Nano Lett.* **2006**, *6*, 84-88.
44. Zhang, W. H.; Hu, X. X.; Zhang, X. B. Dye-doped fluorescent silica nanoparticles for live cell and in vivo bioimaging. *Nanomater.* **2016**, *6*, 81.
45. Wang, C.; Yan, J. Cui, X.; Wang, H. Synthesis of raspberry-like monodisperse magnetic hollow hybrid nanospheres by coating polystyrene template with Fe_3O_4@ SiO_2 particles *J. Colloid Interface Sci.* **2011**, *354*, 94-99.
46. Zheng, J.; Liu, Q.; Wei, W.; Lu, Y.; Wang, S.; Chen, H.; Zhou, Y. Roughness surface of raspberry-shaped silica nanoparticles effect on shear thickening colloidal suspensions. *Appl. Surf. Sci.* **2022**, *606*, 154917.
47. Du, X.; He, J. A self-templated etching route to surface-rough silica nanoparticles for superhydrophobic coatings. *ACS Appl. Mater. Interfaces* **2011**, *3*, 1269-1276.
48. Li, X.; He, J. In situ assembly of raspberry-and mulberry-like silica nanospheres toward antireflective and antifogging coatings. *ACS Appl. Mater. Interfaces* **2012**, *4*, 2204-2211.
49. Zhao, Z. B.; Zhang, D. M.; Meng, Y. F.; Tai, L.; Jiang, Y. One-pot fabrication of fluoride-silica@ silica raspberry-like nanoparticles for superhydrophobic coating. *Ceramics International* **2016**, *42*, 14601-14608.
50. Semeykina, V. S.; Zharov, I. Medium Controlled Aggregative Growth as a Key Step in Mesoporous Silica Nanoparticle Formation. *J. Colloid Interface Sci.* **2022**, *615*, 236-247.
51. ·Vivero-Escoto, J. L.; Slowing, I. I.; Trewyn, B. G.; Lin, V. S-Y. Mesoporous silica nanoparticles for intracellular controlled drug delivery. *Small* **2010**, *6*, 1952-1967.
52. ·Manzano, M.; Vallet-Regí, M. Mesoporous silica nanoparticles for drug delivery. *Adv. Funct. Mater.* **2020**, *30*, 1902634.
53. Feldmann, V.; Engelmann, J.; Gottschalk, S.; Mayer, H. A. Synthesis, characterization and examination of Gd [DO3A-hexylamine]-functionalized silica nanoparticles as contrast agent for MRI-applications. *J. Colloid Interface Sci.* **2012**, *366*, 70-79.
54. Cha, B. G.; Kim, J. Functional mesoporous silica nanoparticles for bio-imaging applications. *Wiley Interdiscip. Rev. Nanomed. Nanobiotechnol.* **2019**, *11*, e1515.
55. Niculescu, V. C. Mesoporous silica nanoparticles for bio-applications. *Front. Mater.* **2020**, *7*, 36.

Preprints (www.preprints.org) | NOT PEER-REVIEWED | Posted: 27 December 2023 doi:10.20944/preprints202312.1842.v1

56. Brozek, E. M.; Zharov, I. Internal Functionalization and Surface Modification of Vinylsilsesquioxane Nanoparticles. *Chem. Mater.* **2009**, *21*, 1451-1456.
57. Tripathi, V. S.; Kandimalla, V. B; Ju, H. Preparation of Ormosil and its Applications in the Immobilizing Biomolecules. *Sens. Actuators B* **2006**, *114*, 1071-1082.
58. Gonçalves, M. C. Sol-gel silica nanoparticles in medicine: A natural choice. Design, synthesis and products. *Molecules* **2018**, *23*, 2021.
59. Soloway, A. H.; Tjarks, W.; Barnum, B. A.; Rong, F.-G.; Barth, R. F.; Codogni, I. M.; Wilson, J. G. The Chemistry of Neutron Capture Therapy. *Chem. Rev.* **1998**, *98*, 1515-1562.
60. Gao, Z.; Moghaddam, S. P. H.; Ghandehari, H.; Zharov, I. Synthesis of Water-Degradable Silica Nanoparticles from Carbamate-Containing Bridged Silsesquioxane Precursor. *RSC Adv.* **8**, 4914-4920 (2018).
61. Gao, Z.; Zharov, I. Large Pore Mesoporous Silica Nanoparticles by Templating with a Nonsurfactant Molecule, Tannic Acid. *Chem. Mater.* **26**, 2030-2037 (2014).
62. Brozek, E. M.; Washton, N. M.; Mueller, K. T.; Zharov, I. Silsesquioxane Particles with Internal Functional Groups. *J. Nanopart. Res.* **19**, 85-97 (2017).
63. Walton, N. I.; Gao, Z.; Zharov, I. Theranostic Anticancer Agents Based on Internally Functionalized ORMOSIL Nanoparticles. *MRS Proceedings* **1526**, 215-221 (2014).
64. Walton, N. I.; Naha, P.; Cormode, D. P.; Zharov, I. Mesoporous Organosilica Nanoparticles with Internal Metal-Chelating Groups: Transition Metal Uptake and Gd^{3+} Relaxivity. *ChemistrySelect* **8**, e202301454 (2023).
65. Ottenbrite, R. M.; Wall, J. S.; Siddiqui, J. A. Self-Catalyzed Synthesis of Organo-Silica Nanoparticles. *J. Am. Ceram. Soc.* **2000,** *83*, 3214-3215.
66. Stöber, W.; Fink, A.; Bohn, E. J. Controlled Growth of Monodisperse Silica Spheres in the Micron Size Range. *J. Colloid Interface Sci.* **1968**, *26*, 62-69.
67. Gu, J.; Fan, W.; Shimojima, A.; Okubo, T. Organic–inorganic mesoporous nanocarriers integrated with biogenic ligands. *Small* **2007**, *3*, 1740-1744.
68. Hartono, S. B.; Gu, W.; Kleitz, F.; Liu, J.; He, L.; Middelberg, A. P. J.; Yu, C.; Lu, G. Q.; Qiao, S. Z. Poly-L-lysine functionalized large pore cubic mesostructured silica nanoparticles as biocompatible carriers for gene delivery. *ACS Nano* **2012**, *6*, 2104-2117.
69. Sing, K. S. Reporting physisorption data for gas/solid systems with special reference to the determination of surface area and porosity. *Pure & Appl. Chem.* **1985**, *57*, 603-619.

Disclaimer/Publisher's Note: The statements, opinions and data contained in all publications are solely those of the individual author(s) and contributor(s) and not of MDPI and/or the editor(s). MDPI and/or the editor(s) disclaim responsibility for any injury to people or property resulting from any ideas, methods, instructions or products referred to in the content.